Light Metals 2012 *Edited by: Carlos E. Suarez*
TMS (The Minerals, Metals & Materials Society), 2012

Light Metals 2012

ALUMINUM REDUCTION TECHNOLOGY

Cell Technology and Operation

SESSION CHAIR
Bjørn Petter Moxnes
Hydro Aluminium
Sunndalsøra, Norway

Light Metals 2012 *Edited by: Carlos E. Suarez*
TMS (The Minerals, Metals & Materials Society), 2012

DX+, AN OPTIMIZED VERSION OF DX TECHNOLOGY

Ali Zarouni, Abdalla Zarouni, Nadia Ahli, Sergey Akhmetov, Ibrahim Baggash, Lalit Mishra, Amal Al Jasmi,
Marwan Bastaki, Michel Reverdy,
Dubai Aluminium Company (DUBAL), PO Box 3627, Dubai, UAE

Keywords: High amperage, DX technology, DX+ technology

Abstract

Since the 1990's, DUBAL has engaged in self-development of proprietary aluminium reduction technology. DX and DX+ technologies, both being in-house designed, modeled, tested and optimized, are the latest products of this development process. In quest to decrease capital cost per tonne, DUBAL designed DX+ technology and started up five demonstration cells between June and August 2010. DX+ cells are similar to DX cells, but larger in size: the productivity per square metre of potroom is increased by more than 17%. This paper describes the DX+ cell design evolution from DX technology. It also summarizes the on-target performance achieved by the DX+ demonstration pots during their first year of operation at 420 kA. DX+ technology has been selected for the EMAL Phase II project. The project FEED study, completed in June 2011, is based on one potline of 444 DX+ pots. The design allows for an operating amperage increase to 460 kA.

Introduction

Over many years of technology development, DUBAL has accumulated a great deal of knowledge and the tools required for in-house development of modern reduction technology. This has enabled the development of technologies to be fast-tracked in the recent past. After successfully implementing DX technology in 40 demonstration cells in DUBAL in 2008, the same technology was installed in the EMAL Phase I project (two potlines with 378 cells each) [1]. Meanwhile, technology development at DUBAL continued. By August 2009, DUBAL completed the design of a newer generation cell design, called DX+. As the name indicates, DX+ technology is an extension of the DX design: it promises the same outstanding performance at lower capital cost per installed tonne of capacity.

DX+ cells were designed to operate at 420 kA initially and are ultimately anticipated to operate at up to 460 kA. Accordingly, DX+ cells are larger than DX cells: the potshell is 0.3 m wider and 0.6 m longer. However, the pot-to-pot distance is 6.3 m, the same as for DX cells. The busbar configuration has also been maintained, but the busbar cross-sectional area in DX+ industrial cells will be larger to accommodate the higher amperage without increase of external voltage drop. While both cells have 36 anodes, the size of the DX+ anode was increased to match greater potshell dimensions and to maintain the current density at higher amperage. Neither DX nor DX+ technology requires forced potshell cooling or external magnetic compensation.

Having developed confidence through modeling and engineering design, five DX+ demonstration cells were installed in DUBAL's Eagle section, replacing the five DX prototype cells. The DX+ cells were energized between June and August 2010. Figure 1 shows a view of the Eagle section that houses the DX+ cells. The cells achieved the desired performance from November 2010 onwards. This allowed DX+ technology to be assessed as "bankable" by the EMAL Phase II lender's technical advisor. Thus, a potline of 444 DX+ cells with a production capacity of 520 000 tonnes per year will be installed at EMAL Phase II and is scheduled for start-up in December 2013.

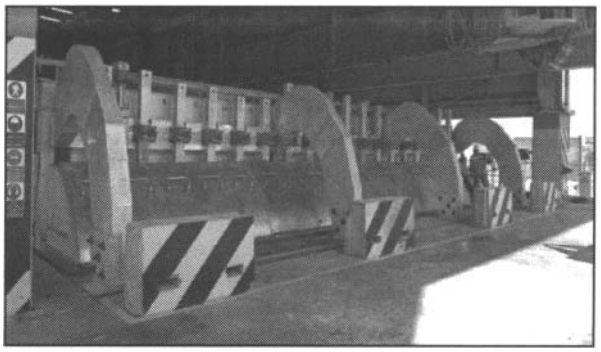

Figure 1. DX+ cells in the Eagle section at DUBAL.

DX+ Design Modeling and Validation

In an effort to optimize DX technology, mathematical modeling and engineering evaluations were carried out. These activities enabled the development of an alternative design, requiring less capital expenditure while maintaining the technical performance of the cells.

At the design stage, models were developed for magneto-hydrodynamic (MHD), thermo-electric and mechanical evaluations of the cell design. MHD modeling included metal heave, metal and bath circulation patterns, magnetic field, and stability analysis. Thermo-electric modeling was used to evaluate the cell heat balance, freeze profile, busbars temperature and current distribution, collector bar current distribution and potshell temperature. Potshell deformation was also studied using mechanical modeling.

The model results were compared to those of DX technology for conformance on acceptable ranges. These models were later validated through data collection from the actual operating DX+ cells. The design validation measurements showed consistent figures compared to those expected from the model results.

In terms of MHD modeling, the metal circulation pattern, shown in Figure 2, and velocities were comparable to those of DX technology. Metal velocity measurements in the DX+ cells also showed similar patterns to those which the model predicted. Metal velocity measurements were taken using iron rods positioned between the anodes on upstream and downstream sides of the cell, as well as at the tap and duct ends. Figure 3 shows a comparison between the model (blue arrows) and actual measurement (red arrows). Except for a few locations, very good agreement was

observed between the two patterns, both in terms of magnitude and direction.

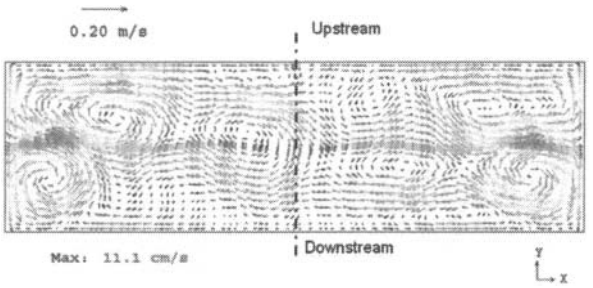

Figure 2. DX+ metal circulation patterns and velocities: modeling results.

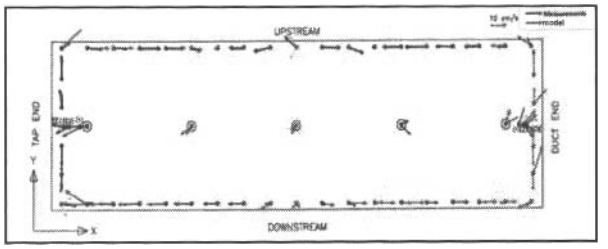

Figure 3. DX+ metal circulation patterns and velocities: modeling (blue arrows) vs. measured (red arrows) results.

Furthermore, stability limits were measured by squeezing the anode-to-cathode distance (ACD) until the cell no longer was stable. The stability analysis showed that at the present operating voltage, DX+ cells have a large margin of ACD above the instability limit. Additionally, the impact of changing anodes on cell stability was analysed and found to be easily mitigated with the pot control system.

From a thermo-electric perspective, the DX+ models showed similar trends in cell heat balance as observed in DX cells. Freeze profile measurements also reflected similar trends to those predicted by the model. Figure 4 shows the freeze profile generated by the model, while Figure 5 plots the measured side freeze averaged for the five DX+ cells from November 2010 to June 2011. The two profiles agree well in shape and thickness. The model predicted a freeze thickness of 5 cm at the metal bath interface, while the measured data gave 4.2 cm.

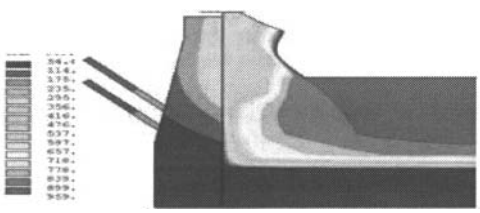

Figure 4. DX+ cathode model showing freeze profile.

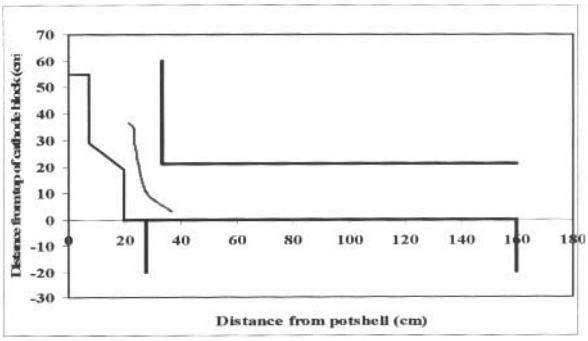

Figure 5. DX+ measured side freeze.

Another important design parameter obtained from the thermo-electric modeling was the collector bar current distribution. Modeling showed an excellent balance between upstream and downstream currents of 50.5% upstream and 49.5% downstream. This compared well with the measured data of 51.3% upstream and 48.7% downstream. Figure 6 shows the current distribution in upstream and downstream collector bars, plotted against the measured current at these locations.

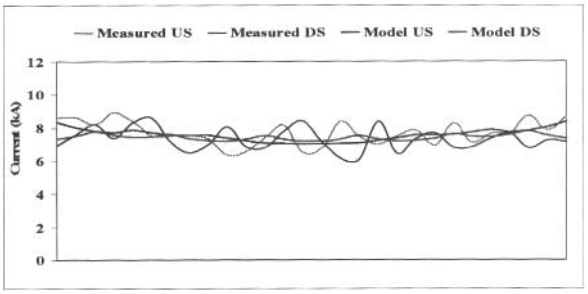

Figure 6. Current distribution in collector bars in DX+ (measured vs. predicted).

Moreover, the potshell temperature was measured at several locations and found to be in general agreement with the modeling results. The potshell design of DX+ is different than the original DX potshell design. The impact of this is reflected in the potshell temperature being on average 25 °C cooler in DX+ cells.

Finally, mechanical models were used to analyze the potshell deformation. Figure 7 shows the model results along with the measurements in the DX+ cells. The model predicted a maximum vertical deflection of 1.3 cm and a maximum horizontal deflection of 3.5 cm. This was very close to the measured data, which showed a maximum vertical deflection of around 1.5 cm and about 3.5 cm (maximum) horizontal deflection.

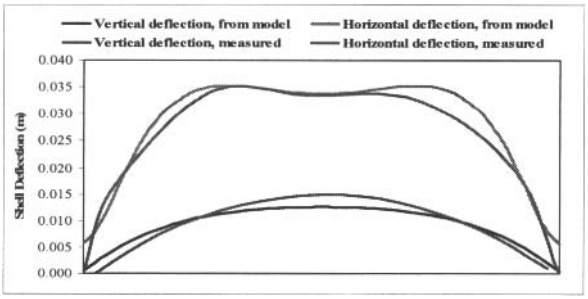

Figure 7. DX+ shell side horizontal and vertical deflections.

DX+: From Design to Demonstration Section

Compared with previous technology development programmes at DUBAL, a new approach was used to fast-track the performance-proving trials. A small, close-knit management development team was used, comprising personnel from Technology Development, Operations and IT. Since all options for improvement were open for consideration, cross-links enabled a very efficient way of testing of new concepts covering all aspects of cell performance. This arrangement resulted in the achievement of outstanding performance parameters in a very short period of time, specifically:

- Cell design: including anode shape, height and yoke assembly design, etc.
- Operating conditions: including fine-tuning of cell operating parameters such as voltage set point and ACD, metal and bath height targets, anode cover thickness, draft rate, etc.
- Work practices: including optimizing the anode setting pattern, anode reference height, cavity cleaning practices, anode covering practices, new anode current distribution adjustment practices, and appropriate span for tapping tables.
- Control strategy: including innovative ways of signal processing, anode effect treatment, and feed and voltage control so that maximum information can be derived to prevent process variations.
- Environmental performance: focusing on better hooding design, draft velocities, and minimization of anode effect duration.

The Eagle section, housing the five DX+ cells, is located at the end of Potline 5, from which it receives more than half of its current. The DX+ cells are numbered 273 to 277 in continuation of the numbering sequence of the 272 cells of Potline 5.

For expediency and time-saving reasons, the DX busbars were retained in the DX+ Eagle demonstration cells, with minor variations to improve cell stability at higher amperage. This is a disadvantage, as the cell-to-cell voltage is higher than it will be in the industrial implementation. Other constraints included using the same service crane, jacking frame, metal crucible, and the space within the building. These factors added some difficulty to the operation of the demonstration cells and the absence of these constraints in industrial design is expected to ease the operation and improve the cell performance.

Key Performance Indicators of DX+ cells

The DX+ key performance indicators exceeded expectations at the target amperage of 420 kA. Table I and Figures 8 to 19 below show the average KPIs for the first six months of 2011. Note that the horizontal scale of the graphs is in weeks of 2011. In Table I, the actual voltage and corresponding specific energy consumption are corrected for the expected improvements due to design changes in the industrial DX+, which include larger busbar cross-sectional areas and anode yoke redesign.

Table I. DX+ Eagle demonstration cells - key performance indicators.

KPI	Units	Average of 5 DX+ cells (January. – June 2011) -	DX+ Industrial (Design criteria)
Amperage	kA	419.6	420 to 460
Current efficiency	%	95.5	> 95.0
Cell voltage	Volts	4.22*	< 4.25
DC Specific energy consumption	kWh/kg Al	13.17*	< 13.33
Net carbon consumption	kg C/kg Al	0.405	< 0.415
Aluminium purity	%	99.93	> 99.89

*Based on 4.35 V actual minus 0.13 V for design changes in the industrial version of DX+.

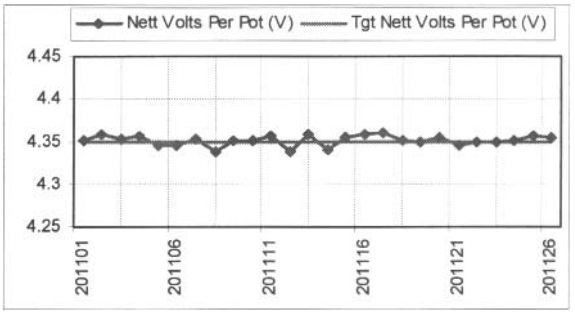

Figure 8. Potline amperage.

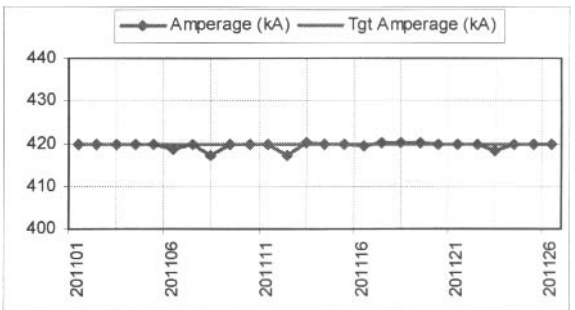

Figure 9. DX+ Eagle cell voltage.

Note that industrial DX+ cell voltage will be 0.13 V lower.

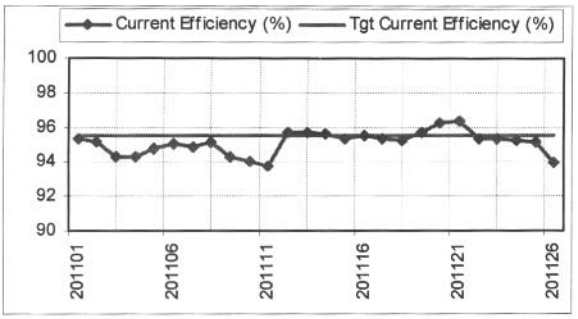

Figure 10. Current efficiency.

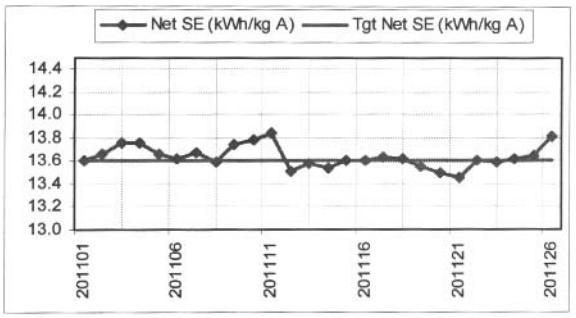

Figure 11. Net specific energy consumption.

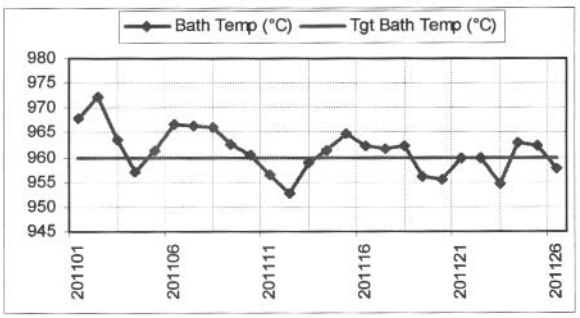

Figure 12. Bath temperature.

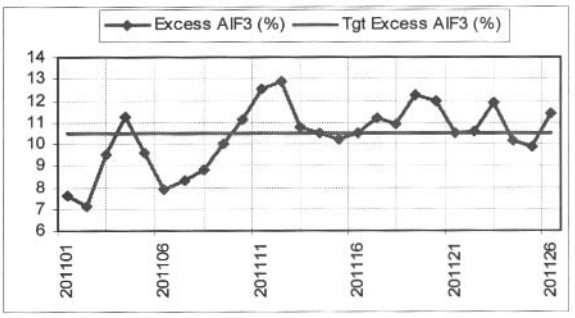

Figure 13. Excess AlF_3.

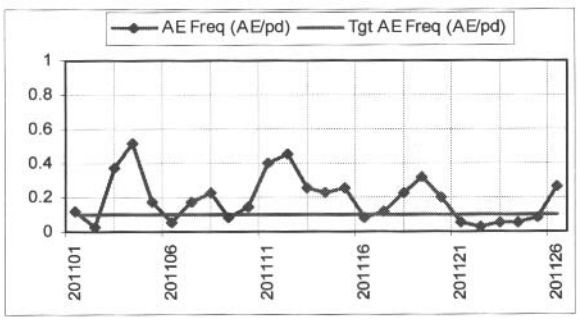

Figure 14. Anode effect frequency.

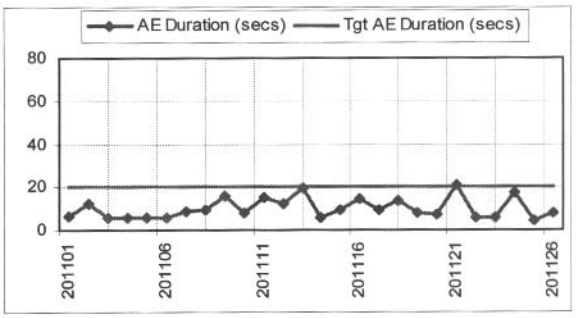

Figure 15. Anode effect duration.

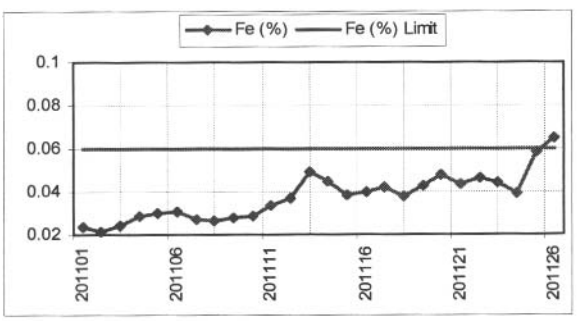

Figure 16. Fe percentage in the metal.

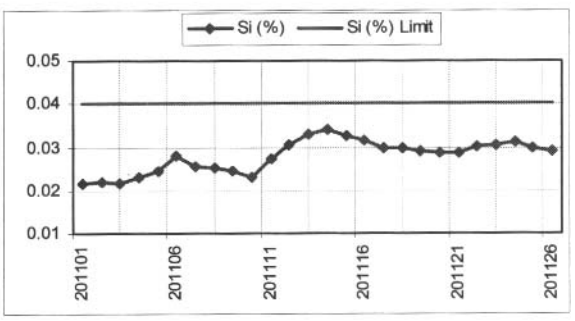

Figure 17. Si percentage. in the metal.

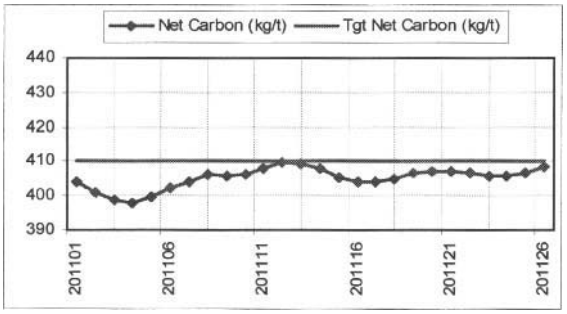

Figure 18. Net carbon consumption.

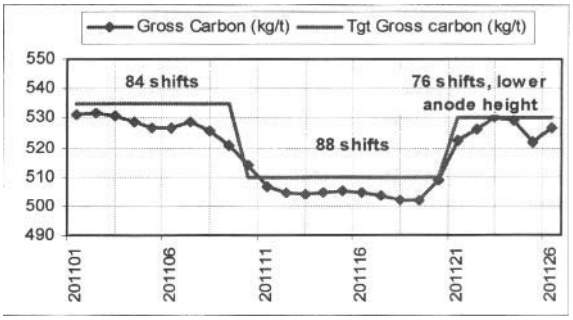

Figure 19. Gross carbon consumption.

Net and Gross Carbon Consumption

During the technology improvement processes, changes were made to control bath height, anode setting and anode covering practices. Every anode butt weight and dimensions were recorded so as to obtain accurate consumption figures and optimize work practices. Typically, more than 80% of the butts from all cells were measured.

Table III shows the average and the best net carbon consumption (NCC) and gross carbon consumption (GCC) for each cell recorded from January to June 2011. The best result for net carbon consumption shows an exceptional 0.392 kg C/kg Al for a moving average of 4 weeks' duration.

Table III. Average and best net and gross carbon consumptions for all DX+ cells.

Cell No.	Average NCC	Average GCC	Best NCC	Best GCC
273	0.404	0.519	0.369	0.502
274	0.406	0.52	0.398	0.503
275	0.406	0.516	0.394	0.496
276	0.408	0.517	0.403	0.502
277	0.408	0.517	0.394	0.503
Avg all	0.406	0.518	0.392	0.501

Anode Effect Performance and PFC Emissions

Like the DX cells the DX+ cells perform very well in terms of PFC emissions. Table II summarizes the anode effect performance and equivalent CO_2 from PFC emissions of the five DX+ Eagle demonstration cells from January to June 2011. Although the average anode effect frequency for the five cells during that period was 0.19 per pot day; the average duration of these anode effects was extremely low, less than 10 seconds. This resulted in a very low calculated PFC emission rate and a corresponding average CO_2 equivalent of 0.033 t/t Al.

PFC emissions and CO_2 equivalent were calculated according to Equations (1) – (3) [2].

$$E_{CO_2-eq} = \frac{GWP_{CF_4} E_{CF_4} + GWP_{C_2F_6} E_{C_2F_6}}{1000} \quad (1)$$

$$E_{CF_4} = S_{CF_4} AEM \quad (2)$$

$$E_{C_2F_6} = E_{CF_4} F_{C_2F_6/CF_4} \quad (3)$$

Where : E_{CO2-eq} = Equivalent emission of CO_2, t/tAl
E_{CF4} = Emission of CF_4, kg/tAl
E_{C2F6} = Emission of C_2F_6, kg/tAl
GWP_{CF4} = Global warming potential of CF_4
GWP_{C2F6} = Global warming potential of C_2F_6
S_{CF4} = Slope coefficient for CF_4, kg CF_4 per tonne of aluminium per anode effect minute per cell day
AEM = anode effect duration, minutes per cell day
$F_{C2F6/CF4}$ = Weight fraction of C_2F_6/CF_4

Table II. Anode effect performance (1 January – 30 June 2011).

Cell No.	Average AE freq. (AE/pd)	Average AE duration (s)	Average AE duration (s/pot-day)	Average CO_2 equiv (t/t Al)
273	0.155	9.1	1.41	0.026
274	0.099	9.5	0.94	0.017
275	0.265	6.8	1.80	0.033
276	0.282	12.2	3.44	0.062
277	0.155	10.2	1.58	0.029
Average	0.191	9.6	1.83	0.033

The values of CO_2 equivalent in Table II were calculated using the Tier 2 method, which uses site specific anode effect data but industry average coefficients. The latter were obtained from [2]: S_{CF4} = 0.143 and $F_{C2F6/CF4}$ = 0.121. The values of global warming potentials of CF_4 and C_2F_6, were obtained from [3]. For Table II, the commonly used values from the Intergovernmental Panel on Climate Change (IPCC) Second Assessment Report (SAR) were used: GWP_{CF4} = 6500 and GWP_{C2F6} = 9200. However these values have been revised by the IPCC Fourth Assessment Report (AR4) to 7390 for CF_4 and 12200 for C_2F_6.[3] Using these figures would increase the CO_2 equivalent by approximately 17% over the values reported in Table II.

It is also possible to calculate the CO_2 equivalent by the Tier 3 method, which uses site specific anode effect data and coefficients based on local facility measurements of PFCs [2]. Measurements of PFC emissions in DX+ cells were made in December 2010 and January 2011 and gave an average CO_2 equivalent of 0.045 t/tAl, which is higher than the value in Table II. This is due to S_{CF4} being greater than the Tier 2 values. Measurements have also

shown that at these very low PFC emissions, there are also non-negligible non-anode effect PFC emissions [4].

Metal Purity

DX+ cells yield good metal purity. Table IV shows the iron and silicon contents for the five DX+ cells, together with the aluminium percentage. An increase in iron content to 0.06%, observed at the end of June (weeks 25 and 26), was due to minor stub washes. The increase in Si content from approximately 0.02% to 0.03% was due to change in the raw materials used. The average purity of the metal produced was 99.93%.

Table IV. Average Fe%, Si% and Al% for DX+ cells.

Cell No.	Avg. Fe %	Avg. Si %	Avg. Al %
273	0.038	0.028	99.931
274	0.033	0.028	99.936
275	0.035	0.028	99.933
276	0.032	0.027	99.938
277	0.044	0.030	99.923
Average	0.036	0.028	99.932

EMAL Phase II

EMAL Phase II FEED (Front End Engineering and Design) was carried out by SNC Lavalin during the first half of 2011, with the support of the EMAL Project and Operation teams and the involvement of DUBAL for the reduction area. Following a feasibility study completed in December 2010, the FEED study was based upon the implementation of DX+ technology in a third potline comprising 444 cells. The FEED report was completed and issued at the end of June 2011 with the EPCM (Engineering, Procurement, Construction and Management) contract awarded to SNC Lavalin at the beginning of July 2011. The nominal capacity of EMAL Potline 3 will be 520 000 tonnes per year at 420 kA. However, the design of the substation will allow up to 460 kA and the total capacity of EMAL smelter is thus expected to reach close to 1.4 million tonnes per year, boosted by the roll-out of second generation cathode design in the existing Phase I (potlines 1 and 2) and full amperage creep.

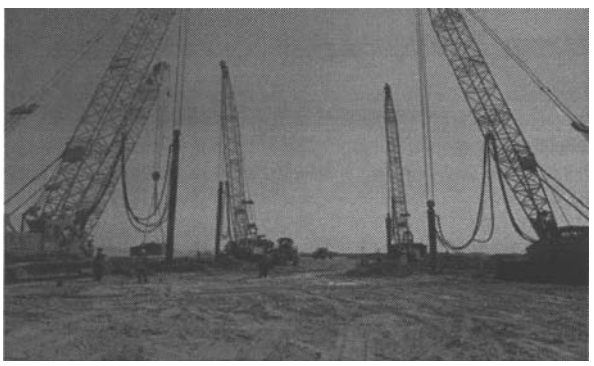

Figure 20. EMAL Phase II construction site (October 2011).

Conclusion

The rapid progression of DX+ technology from conception, through modeling and design, to the demonstration phase has facilitated the choice of DX+ technology for industrial implementation in a very short period of time. DX+ technology, by building on DX technology, is achieving world-class operational performance as a result of considerable analysis and optimization activities. DX+ technology achieves similar outstanding operational performances as DX technology, with the added advantage of higher productivity and lower capital cost per installed tonne of capacity.

Acknowledgements

Throughout the development, demonstration and industrial implementation of DX+ technology, there have been many people who are not mentioned in the author list, but who made valuable contributions to the success of these projects.

Special thanks go to Prof. Barry Welch, Dr. Vinko Potocnik and Jeffrey Keniry, for their continuous input and advice during the design and performance enhancement programme throughout this project.

References

1. Ali Al Zarouni et al., "The Successful Implementation of DUBAL DX Technology at EMAL", Light Metals 2012.
2. IAI, "The Aluminium Sector Green House Gas Protocol (Addendum to WRI/WBCSD Green House Gas Protocol), Green House Gas Emissions and Monitoring for Aluminium Industry", (October 2006, http://www.world-aluminium.org - Downloads).
3. IPCC, "Fourth Assessment Report: Climate Change 2007, Working Group 1: The Physical Science Basis, 2.10.2 Direct Global Warming Potentials".
4. Abdalla Al Zarouni and Ali Al Zarouni, "Dubal's Experience of Low Voltage PFC Emissions", Proceedings of the 10th Australasian Aluminium Smelting Technology Conference, Launceston, Australia, 9th to 14th October 2011, Editors Barry Welch et al.